

## Photophysics and Photochemistry of 1-Nitropyrene

Rafael Arce,\* Eduardo F. Pino, Carlos Valle, and Jesús Ágreda†

Department of Chemistry, University of Puerto Rico, Rio Piedras Campus, San Juan, Puerto Rico 00931-3346

Received: April 8, 2008; Revised Manuscript Received: July 24, 2008

1-Nitropyrene (1NPy) is the most abundant nitropolycyclic aromatic contaminant encountered in diesel exhausts. Understanding its photochemistry is important because of its carcinogenic and mutagenic properties, and potential phototransformations into biologically active products. We have studied the photophysics and photochemistry of 1NPy in solvents that could mimic the microenvironments in which it can be found in the atmospheric aerosol, using nanosecond laser flash photolysis, and conventional absorption and fluorescence techniques. Significant interactions between 1NPy and solvent molecules are demonstrated from the changes in the magnitude of the molar absorption coefficient, bandwidth at half-peak, oscillator strengths, absorption maxima, Stokes shifts, and fluorescence yield. The latter are very low ( $10^{-4}$ ), increasing slightly with solvent polarity. Low temperature phosphorescence and room temperature transient absorption spectra demonstrate the presence of a low energy  $^3(\pi, \pi^*)$  triplet state, which decays with rate constants on the order of  $10^4$ – $10^5$   $s^{-1}$ . This state is effectively quenched by known triplet quenchers at diffusion control rates. Intersystem crossing yields of 0.40–0.60 were determined. A long-lived absorption, which grows within the laser pulse, and simultaneously with the triplet state, presents a maximum absorption in the wavelength region of 420–440 nm. Its initial yield and lifetime depend on the solvent polarity. This species is assigned to the pyrenoxy radical that decays following a pseudo-first-order process by abstracting a hydrogen atom from the solvent to form one the major photoproducts, 1-hydroxypyrene. The  $^3(\pi, \pi^*)$  state reacts readily ( $k \sim 10^7$ – $10^9$   $M^{-1} s^{-1}$ ) with substances with hydrogen donor abilities encountered in the aerosol, forming a protonated radical that presents an absorption band with maximum at 420 nm.

### Introduction

Thousands of tons of polycyclic aromatic hydrocarbons (PAHs) are released annually into the atmosphere as a result of the incomplete combustion of fossil fuels and other organic matter in anthropogenic activities.<sup>1</sup> The main contributors of PAHs and nitroPAHs in urban air are considered to be automobiles, domestic heating systems such as furnaces and kerosene heaters, power incinerators, steel, aluminum, and iron factories, coke oven emissions, and coal burning for industrial and domestic purposes.<sup>2,3</sup> These emissions are likely to increase with the consumption of even more petroleum and coal, especially in developing countries.

Most nitroPAHs are formed by direct combustion processes and emitted from diesel engine vehicles.<sup>4,5</sup> In addition to these sources, heterogeneous or homogeneous reactions of the parent PAHs with OH radicals and nitrogen oxides under photochemical conditions have been reported to form 2-nitropyrene and 2-nitrofluoranthene.<sup>6</sup> Once released into the atmosphere, many nitroPAHs are highly persistent in the environment and can be transported long distances from their original sources. Nitro-pyrenes exist almost entirely in the particle phase under ambient conditions.<sup>7</sup> Human exposure through inhalation of persistent nitroPAHs in the atmospheric particulate phase could lead to serious respiratory and cardiovascular health problems, and higher urban death rates.<sup>8,9</sup> Although nitroPAHs are less abundant in ambient air than PAHs (in the ng/g range),<sup>10,11</sup> about 1–3 orders of magnitude lower, some of them could be more mutagenic and carcinogenic than their parent PAH.<sup>12–16</sup>

Understanding the reactions and sinks of particle-bound genotoxic and mutagenic nitroPAHs is essential to assess the associated environmental exposure and risks. The transformation of the nitroPAHs in the atmosphere is still debated and knowledge of their fates in the environment is still of interest and required. The principal degradation route for nitroPAHs found in the atmospheric particulate matter appears to be photolytic degradation.<sup>17–19</sup> Possible heterogeneous reactions with  $O_3$  and  $N_2O_5$  have also been postulated, although these do not represent an important degradation route.<sup>19</sup> Furthermore, there is evidence that the composition of the organic layer of an aerosol surrounding the elemental carbon core influences strongly the photochemical transformations of PAHs.<sup>20–25</sup>

Several independent investigators have examined the photochemistry of 1-nitropyrene in solvents such as methanol,<sup>26</sup> 2-propanol,<sup>27</sup> benzene,<sup>28</sup> dimethyl sulfoxide,<sup>29</sup> acetonitrile,<sup>30–32</sup> cyclohexane, and glycerine,<sup>24,25</sup> with the objective of mimicking the complex environment of the atmospheric aerosol. Products such as hydroxypyrene,<sup>24,26</sup> nitrohydroxypyrene,<sup>26,29,31</sup> pyrene-diones,<sup>28</sup> and pyrene<sup>26</sup> have been reported. The formation of many of these<sup>26</sup> can be explained in terms of an initial nitro to nitrite rearrangement mechanism involving an upper excited  $n, \pi^*$  triplet state, as originally proposed by Chapman and co-workers for the photochemistry of 9-nitroanthracene.<sup>32</sup>

It is expected that nitroPAHs, as well as other PAHs, interact with a wide variety of organic components encountered within the atmospheric aerosols, and that these organic compounds affect their photochemical processes.<sup>20–25</sup> Photodegradation rates for 1-nitropyrene dissolved in cyclohexane, diisooctylphthalate, and glycerine, were reported by Fieldberg and Nielsen.<sup>24,25</sup> Cosolutes such as phenols, substituted phenols, benzaldehydes, and oxyPAHs, known constituents of wood smoke or diesel

\* Corresponding author. E-mail: rarce@uprr.pr.

† Universidad Nacional de Colombia, Bogota.

particles, accelerated the photodegradation rates. For phenols they proposed a reaction sequence that involves the hydrogen abstraction from the phenolic hydrogen by an excited nitroPAH triplet state leading to unstable intermediates that further transform into products. These other intermediates were not identified.

Few studies have been carried out on the identification and kinetics of the reactive intermediates that participate in the photodecomposition of 1-nitropyrene, although for nitroanthracenes nanosecond to subpicosecond time-resolved transient studies have been reported.<sup>33–36</sup> The 347.2 nm laser photolysis of nitropyrene<sup>37</sup> in benzene, *n*-hexane, ethanol, and ethanol–water solutions resulted in transient absorption spectra with structured absorption in the visible wavelength region (420–650 nm) assigned principally to the lowest triplet state. A triplet molar absorption coefficient and quantum yield of 9300 M<sup>-1</sup> cm<sup>-1</sup> and 0.6 in benzene were reported. A red shift of the spectrum was observed with increasing polarity. The triplet state decayed through a second-order process. A long-lived intermediate ( $\tau_{1/2} = 15 \mu\text{s}$ ) was observed in oxygen containing solutions. From a series of laser photolysis studies of 9-nitroanthracene and other meso-substituents in solution, Hamanoue and co-workers<sup>33–36</sup> have proposed the following mechanism. After laser excitation of nitroanthracene to the first excited-singlet state, this state rapidly decays (0.8 ps) by two competing channels. The first one leads to its rearrangement to an unidentified intermediate or an aryl nitrite that transforms into an aryloxy radical and NO. The second channel leads to a higher energy triplet state that decays into the lower phosphorescence state. Peón and co-workers<sup>38</sup> concluded from anisotropy measurements using femtosecond fluorescence up-conversion that no significant internal conversion occurs in the singlet excited manifold ( $S_1$ ) of 1-nitropyrene after excitation. They also concluded that fluorescence decay from the  $S_1$  state occurs in a biexponential mode, with an initial larger component with a lifetime on the order of hundreds of femtoseconds and a second component that decays in the 4–6 ps range. The time constants supported an ultrafast intersystem crossing process to an upper triplet state as the principal pathway for the  $S_1$  deactivation. Femtosecond broadband transient absorption spectroscopy measurements combined with ground-state and excited-state calculations provide evidence for the presence of three intermediates.<sup>39</sup> These have been assigned to the Franck–Condon excitation, the relaxed singlet excited state, and lowest triplet state. Theoretical results support a small energy gap between  $S_1(\pi, \pi^*)$  state and a  $T_1(n, \pi^*)$  triplet resulting in a large spin–orbit coupling between these two states and an ultrafast intersystem crossing.

In this paper, we have revisited the ground-state absorption, the first singlet excited state, and the phosphorescence properties of 1-nitropyrene in a series of polar, polar aprotic, and nonpolar solvents. We also studied the reactive intermediates species of INPy in those solvents using the nanosecond laser (266 and 355 nm) photolysis. Our aims were (1) to determine the effect of solvents on photophysical parameters of the singlet and triplet states, (2) to observe the effect of triplet quenchers and hydrogen donors, present in the atmospheric aerosol, on the decay kinetics of the triplet state, and (3) to identify and characterize additional intermediate species such as the pyrenoxy radical, and the radical formed from the hydrogen atom abstraction reaction of the triplet state.

### Experimental Section: Solvents and Reactants

1-Nitropyrene 99%, ferrocene laboratory grade, perylene 99+%, benzophenone 99+%, phenol, 1,2-dihydroxybenzene

(catechol), 1,4-dihydroxybenzene (hydroquinone)  $\geq 99\%$ , 1,2,4-trihydroxybenzene (hydroxyhydroquinone) 99%, 4-hydroxy-3-methoxybenzoic acid (vanillic acid) 97%, 2,6-dimethoxyphenol (syringol) 99%, 4-hydroxy-3-methoxybenzaldehyde (vanillin), 3-methoxy-4-hydroxyphenyl acetic acid (homovanillic acid), 1-hydroxynaphthalene (1-naphthol), and 2-hydroxynaphthalene (2-naphthol) 99% were from Sigma-Aldrich Chemical Co.

Solvents such as benzene  $\geq 99.9\%$  (HPLC grade), cyclohexane 99+%, 3-methylpentane 99+%, carbon tetrachloride (CCl<sub>4</sub>)  $\geq 99.9\%$  (HPLC grade) and 2-propanol 99.5% were from Sigma-Aldrich Chemicals and used as received. Methanol and acetonitrile were obtained from Fisher Scientific. Diethyl ether 99% (HPLC grade), ethyl acetate 99.8% (HPLC grade) and isopentane 99+%, were from Alfa Aesar.

1-Nitropyrene was recrystallized three times from methanol. In this process a noticeable color change from an orange to bright yellow was observed. Its purity was assessed from the emission spectrum of the purified substance in methanol in a Varian Cary Eclipse fluorescence spectrophotometer. Purified 1-nitropyrene in methanol was excited at 355 nm (excitation slit, 5 nm/emission; slit, 10 nm) and the purity was confirmed by the absence of the emission bands at 395 and 405 nm characteristic of 1-hydroxypyrene, a major impurity.

Absorption spectra of INPy in different solvents and purged with N<sub>2</sub> for 30 min were recorded with a Varian Cary IE UV–visible spectrophotometer. The solutions were contained in 1 cm optical path quartz cells closed with a septum. Molar absorption coefficients ( $\epsilon_{\text{max}}$ ) were calculated using the Beer–Lambert law. The bandwidth at half-peak height ( $\Gamma$ ) and the oscillator strengths ( $f$ ) were calculated with the GRAMS AI version 7.01 Thermo Galactic 1991–2002 program, after simulating the nitro group absorption band with a minimal number of five Gaussian curves. From these and the area under the curve, the bandwidth at half-peak height and oscillator strengths were calculated.

Emission spectra of solutions with absorbances ranging from 0.10 to 0.45 were recorded in the fluorometer. Plots of the area under the emission spectra as a function of  $1 - 10^{-A}$ , where  $A$  is the absorbance at the excitation wavelength, were prepared to determine the relative fluorescence quantum yields. Fluoranthene ( $\phi_f = 0.35^{40}$ ) was used as the standard. To determine the emission yield, the following equation was used:

$$\frac{\phi_{\text{flu}}^{\text{unknown}}}{\phi_{\text{flu}}^{\text{standard}}} = \frac{n_{\text{unknown}}^2 \text{Area}_{\text{unknown}} (1 - 10^{-A})_{\text{standard}}}{n_{\text{standard}}^2 \text{Area}_{\text{standard}} (1 - 10^{-A})_{\text{unknown}} K} \quad (1)$$

where the ratio  $\text{Area}/1 - 10^{-A}$  was obtained from the slope of the plots. In this equation,  $n$  is the refractive index of the solvent used, and  $K$  is a factor to correct for the fact that the emission intensity of the standard was recorded using identical emission, excitation slit, and photomultiplier voltage (900 V) as the sample, but with a neutral density filter ( $A = 2.0$ ) in front of the emission slit.

The phosphorescence spectra of INPy in 3-methylpentane, EPA (a mixture of diethyl ether, isopentane and ethanol in 5:5:2 by volume proportion), and diethyl ether glasses were recorded at 77 K. The solutions were poured in a quartz tube with a 4 mm inside diameter and inserted into an optical Dewar flask containing liquid N<sub>2</sub> inside of the phosphorescence accessory of the fluorescence spectrophotometer.

Transient intermediates were generated and studied by laser flash photolysis (LFP) using the third (355 nm, maximum energy of 150 mJ) or fourth (266 nm maximum energy of 70 mJ) harmonic output from a Surelite Nd: YAG laser (Continuum)

as the excitation source<sup>41,42</sup> at room temperature. The sample solutions contained in a 1 cm path length were bubbled with nitrogen or oxygen for at least 30 min prior to irradiation. The intensity of the incident beam (12 ns pulse duration) was attenuated by adjusting the amplifier flash lamp voltage. Transient species were monitored at right angles to the laser beam using a 300 W xenon arc lamp (Oriol Corp.) as the probe light. The light passing through a cuvette (1 cm optical pass length), was detected by a monochromator and photomultiplier (Hamamatsu R928) that completed the system. The output signal was recorded on a digital oscilloscope (LeCroy 9360, 600 MHz, 5 Gs/s) and transferred to a personal computer. The signal was averaged over 30 shots. The sample solution was changed after 300 laser shots to avoid for the excitation of photoproducts and photodegradation of the sample. The energy of the laser was measured with a Newport 1835 high-power meter, or using benzophenone as an actinometer.

The molar absorption coefficient of the triplet–triplet absorption ( $\epsilon_T$ ) of INPy was measured by the energy-transfer method.<sup>43</sup> Perylene was used as triplet energy acceptor for the determination of  $\epsilon_T$  of the INPy triplet in nonpolar and polar environments. Using the molar absorption coefficient of triplet state of INPy and benzophenone as an actinometer in acetonitrile, we determined the power dependence of the transient absorption signals for the triplet state of the actinometer, and for the INPy at a wavelength where the molar absorption coefficients of the triplet states were known. Optically matched solutions at the excitation wavelength were used. From these plots the triplet quantum yield of INPy was calculated using<sup>2,44</sup>

$$\phi_{\text{unknown}} = \frac{\text{slope}_{\text{unknown}}}{\epsilon_{\text{unknown}}} \frac{\epsilon_{\text{standard}}}{\text{slope}_{\text{standard}}} \phi_{\text{standard}} \quad (2)$$

In quenching experiments using ArOH in nonpolar (cyclohexane) and polar (acetonitrile and 2-propanol) solvents the concentration of INPy was  $\sim 10^{-5}$  M and the cosolute concentration ranged  $(1-5) \times 10^{-3}$  M. Quenchers were added as aliquots of fresh standard solutions. In all cases, the solvents were used from freshly-opened bottles.

## Result and Discussion

**Ground-State Properties.** Depending on the solvents, Figure 1 depicts absorption spectra obtained in nonpolar and polar solvents, the UV–visible absorption spectrum of INPy consist of three major bands with maxima around 233 (not shown in Figure 1), 285–295, and 365–405 nm. The onset of the long wavelength band (not observed in the pyrene spectrum, the parent PAH) shifted toward the red in polar solvents relative to the spectrum in nonpolar hexane. This band's vibronic structure is partially lost in polar solvents, due to strong interactions between the excited-state and solvent molecules. The intensity of the vibronic transitions decreased with increasing wavelength in nonpolar solvents, but the opposite was observed in polar solvents. This may be due to an increase of the intensity in symmetry forbidden vibrational components on that band that increased with solvent polarity.<sup>45</sup> The long-wavelength band is typical of nitropyrenes, and results from  $\pi, \pi^*$  transitions associated with the  $\text{NO}_2$  group.<sup>26,27,46</sup> The calculated molar absorption coefficients ( $\epsilon_{\text{max}}$ ), bandwidth at half-peak height ( $\Gamma$ ), and oscillator strengths ( $f$ )<sup>47</sup> for the red-most band are included in Table 1 and were similar to those reported in hexane,<sup>29</sup> benzene,<sup>37</sup> and methanol.<sup>26,46</sup> The oscillator strengths were on the order of 0.13–0.16 and showed a small increase in nonpolar solvents. Bandwidths were greater in polar solvents. Taken together, these results indicated strong interactions between the

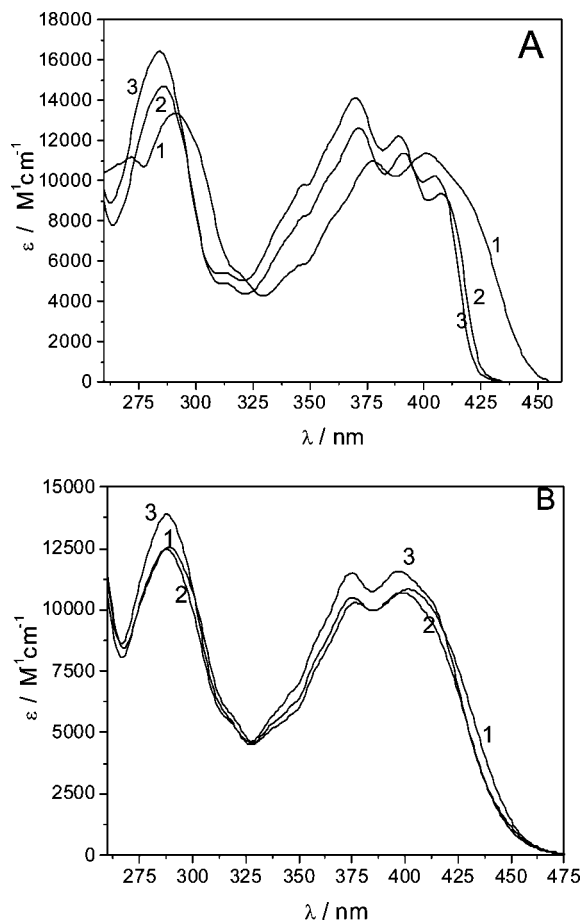


**Figure 1.** Absorption spectra at room temperature for INPy in (A) nonpolar: (1) benzene, (2) cyclohexane, (3) 3-methylpentane; and (B) polar: (1) acetonitrile, (2) methanol, and (3) 2-propanol.

**TABLE 1: Ground-State Properties Associated with the Nitro-Band of 1-Nitropyrene at Room Temperature**

solvent	diel <sup>a</sup>	$\lambda_{\text{max}}$ /nm	$\epsilon_{\text{max}}/\text{M}^{-1}\text{cm}^{-1}$	$f$	$\Gamma/\text{cm}^{-1}$
3-methylpentane	1.9	348 (s), <sup>b</sup> 370	9809/14136	0.164	4917
		389, 404	12236/10212		
hexane	2.0	347 (s), 370	8986/13226	0.156	4833
		389, 405	11565/9692		
methylcyclohexane	2.0	371, 390	13770/12305	0.159	4833
		408	10052		
cyclohexane	2.0	347 (s), 371	8207/12630	0.145	4833
		391, 407	11392/9348		
benzene	2.3	377, 401	10978/11356	0.131	4250
$\text{CCl}_4$	2.3	374, 395	13629/12923	0.158	4667
		411 (s)	10746		
toluene	2.4	377, 401	11176/11489	0.135	4250
dichloromethane	9.1	379, 405	12030/13182	0.163	4667
2-propanol	18.3	375, 397	11494/11572	0.146	4750
<i>n</i> -propanol	20.1	375, 397	11268/11383	0.137	4750
ethanol	24.3	375, 398	10454/10560	0.129	4750
methanol	32.6	375, 399	10511/10698	0.139	4750
acetonitrile	37.5	377, 402	10276/10834	0.137	4750

<sup>a</sup> Dielectric constant U.A. <sup>b</sup> s = shoulder.

electrons associated with the  $\pi, \pi^*$  transition in the  $\text{NO}_2$  group and solvent molecules.

**Singlet-Excited State.** Depending on the solvent, 1-nitropyrene showed a broad, low intensity emission band with maximum in the 430–500 nm wavelength region (Figure 2). A singlet-state energy between 270 and 298  $\text{kJ mol}^{-1}$  was calculated from the intersection of the excitation and emission spectra. The fluorescence emission yields were on the order of  $10^{-4}$  and showed a moderate solvent dependence, which increased with solvent polarity. Stokes shifts (Table 2) increased

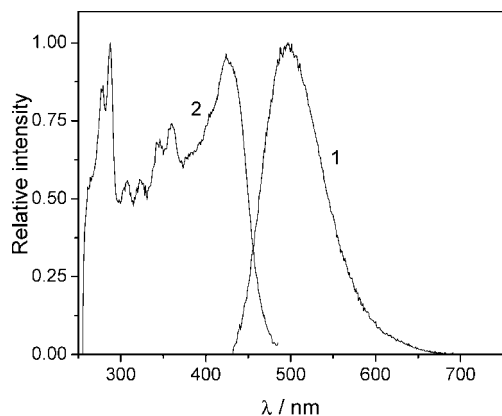


**Figure 2.** Normalized fluorescence spectra of 1NPy in dichloromethane ( $\text{CH}_2\text{Cl}_2$ ) at room temperature. (1) Fluorescence emission spectrum, excitation wavelength 370 nm. (2) Excitation spectrum, excitation wavelength 475 nm.

with solvent polarity, showing a large dipole moment in the excited state and the  $(\pi, \pi^*)$  character of this state. The low fluorescence yield has been ascribed to an efficient intersystem crossing from the lowest excited-singlet state to an upper triplet ( $n, \pi^*$ ) state, and to the considerable charge-transfer character of this transition.<sup>48</sup> Recent femtosecond transient absorption results demonstrate that the 1NPy singlet excited state relaxes through an ultrafast rotation of the nitro group, which then intersystem crosses with a time constant of 7 ps.<sup>39</sup> Furthermore, the first short fluorescence lifetime observed by Peón et al.<sup>38</sup> was assigned to the ultrafast conformational relaxation of the  $\text{NO}_2$  in the lowest excited singlet state.

**Phosphorescence Spectra in Different Glasses at 77 K.** At 77 K, the phosphorescence emission spectra of 1NPy in 3-methylpentane, EPA, and diethyl ether glasses showed two or three maxima: one at 640 nm, the highest, and two side bands at 700 and 775 nm (Figure 3). Similar spectra have been reported for 1NPy<sup>46</sup> and for other nitroaromatics such as 9-nitroanthracene, with band maxima at 685 and 760 nm in EPA.<sup>49</sup>

The first maximum at 640 nm ( $187 \text{ kJ mol}^{-1}$ ) was very close to the estimated value of  $190 \text{ kJ mol}^{-1}$  for the lowest triplet state obtained by energy-transfer techniques.<sup>37</sup> The energy separation of ( $100 \text{ kJ mol}^{-1}$ ) between the  $S_1$  ( $\pi, \pi^*$ ) and the lowest triplet ( $\pi, \pi^*$ ) state suggested the existence of other triplet states near the  $S_1$  state, as seen in nitroanthracene<sup>34</sup> and nitronaphthalene<sup>50</sup> derivatives and by our recent calculations.<sup>39</sup> In these glasses, phosphorescence lifetimes on the order of 54 ms were determined with monoexponential fit and were similar to those reported for 9-nitroanthracene (14.3 ms).<sup>34,49</sup> These are typical phosphorescence lifetimes of  $\pi, \pi^*$  triplet states of nitroaryl molecules.<sup>51</sup> Thus, the lowest triplet of 1NPy was assigned to a  $^3(\pi, \pi^*)$  state.

**Transient Absorption Spectra.** The 266 or 355 nm laser induced transient spectra (from 5 to 50 mJ) of  $\text{N}_2$  or He-saturated solutions of 1NPy in aprotic and protic polar and nonpolar solvents are shown in Figure 4. In nonpolar solvents absorption maxima occurred in the 440–465, 510–520, and 550–560 nm wavelength regions. A shoulder at 600 nm can also be observed in some of the solvents (benzene,  $\text{CCl}_4$ , and 2-propanol). The transient spectra extended above 700 nm. In polar solvents, a small red shift of 5–10 nm was detected. The initial ratio of the relative intensity of the 440 nm band to the 525 nm band was larger in nonpolar than in polar solvents. In all solvents, the negative absorbances in the transient spectra between 325 and 430 nm were associated with the bleaching of the ground state of 1NPy. In polar solvents, the decay rate of the absorbance

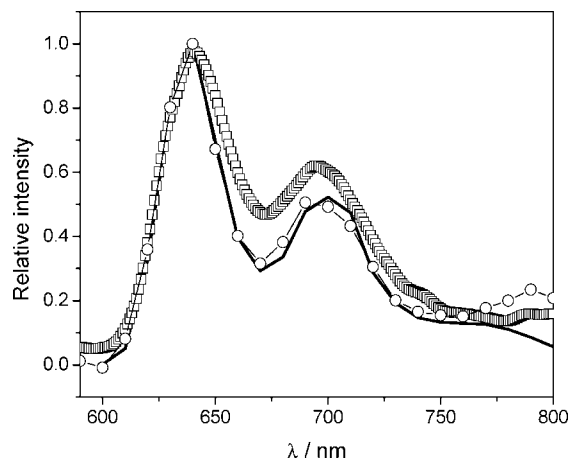


**Figure 3.** Phosphorescence spectra of 1NPy ( $2 \times 10^{-5} \text{ M}$ ) in (—) EPA, (□) 3-methylpentane, and (○) diethyl ether at 77 K. Excitation wavelength 400 nm.

**TABLE 2: Fluorescence Parameters of 1-Nitropyrene at Room Temperature**

solvent	$\lambda_{\text{max}}/\text{nm}$	Stokes shift/ $\text{cm}^{-1}$	$E_0/\text{kJ mol}^{-1}$	$\Phi_{\text{fl}}/10^{-4}$	
3-methylpentane	427	(360) <sup>a</sup>	1333	293	<1
methyl-cyclohexane	430	(360)	1254	290	<1
cyclohexane	425	(360)	1041	291	<1
benzene	465	(370)	3433	279	$1.4 \pm 0.1$
$\text{CCl}_4$	460	(360)	3902	281	<1
toluene	455	(370)	2960	281	$1.2 \pm 0.3$
dichloromethane	495	(370)	4489	271	$3.4 \pm 0.2$
<i>n</i> -propanol	475	(375)	4136	281	$2.6 \pm 0.2$
2-propanol	465	(375)	3681	277	$2.6 \pm 0.4$
ethanol	480	(375)	4293	279	$2.7 \pm 0.3$
methanol	485	(375)	4444	280	$3.4 \pm 0.4$
acetonitrile	500	(375)	4876	275	$2.4 \pm 0.1$

<sup>a</sup> Excitation wavelength.

at 525 nm was faster than in the 400–440 nm region, suggesting the presence of more than one decaying species. A long-lived species (discussed below), with a sharp absorption band in the 400–460 nm region, was observed in all solvents (Figures 5 and 6) after the rest of the absorption bands had disappeared. This band was more clearly observed in polar solvents and at high laser energies ( $>20 \text{ mJ}$  pulses). Figure 6 shows the transient spectrum of 1NPy in cyclohexane at high laser energy (50 mJ) and long observation times.

The initial transient absorption spectra were similar to those observed by Scheerer and Henglein<sup>37</sup> in ethanol, ethanol–water, hexane, and benzene. These were assigned<sup>37</sup> to transitions of the lowest 1NPy triplet state ( $\pi, \pi^*$ ). This assignment was verified by adding known triplet quenchers<sup>52,53</sup>  $\text{O}_2$ , perylene ( $E_T \sim 150 \text{ kJ mol}^{-1}$ ), and ferrocene ( $E_T \sim 167 \text{ kJ mol}^{-1}$ ), and observing an increase in the decay rate in the transient absorption bands in the wavelength region from 530 to 570 nm where only the triplet state absorbs. In the presence of these quenchers the decay of the absorbance fitted a monoexponential function. The triplet yield, measured from the initial triplet absorbance, was not affected by the concentration of the quencher, suggesting the absence of a ground or excited-state complex between 1NPy and the quencher (Table 4).

Calculated quenching rate constants were on the order of diffusion limited ( $10^9$ – $10^{10} \text{ M}^{-1} \text{ s}^{-1}$ ) (Table 3) in nonpolar and polar environments, indicating an energy-transfer process from the lowest 1NPy triplet state to the quencher.

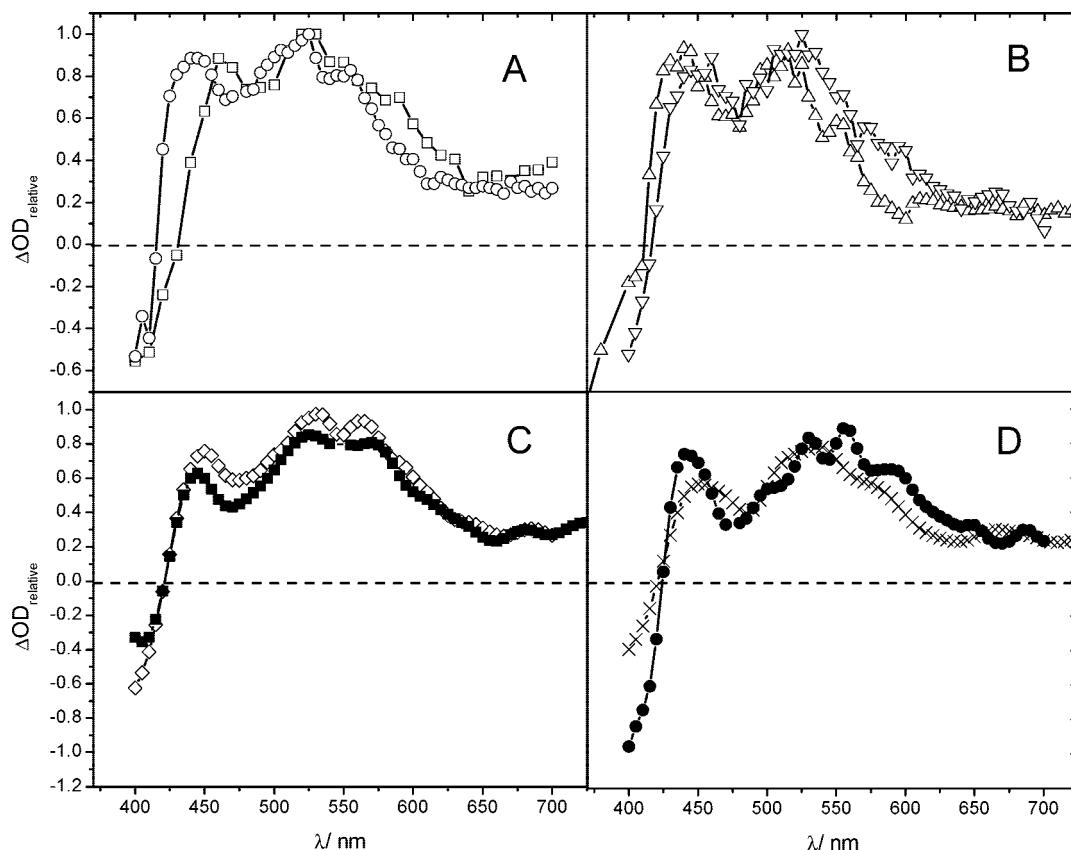


**Figure 4.** Normalized transient absorption spectra of 1NPy ( $6 \times 10^{-5}$  M) at short ( $t = 0.8 \mu\text{s}$ ) observation times in nonpolar and polar solvents: (A) (□) benzene and (○) cyclohexane; (B) (Δ) 3-methylpentane and (∇)  $\text{CCl}_4$ ; (C) (◇) acetonitrile and (■) methanol; (D) (●) 2-propanol and (×) EPA.

The decay rate of the long-wavelength band also depended on the concentration of the 1NPy ground state. The observed first-order rate constants obtained from the decay of the absorbance in the 530–570 nm wavelength region were plotted as a function of the ground-state concentration, assuming a Stern–Volmer relationship. This relationship should follow a straight line, according to  $k_{\text{obs}} = k_0 + k_{\text{sq}}[1\text{NPy}]$ , where  $k_0$  and  $k_{\text{sq}}$  are the decay rate of  $^3(1\text{NPy})$  in an infinitely diluted solution, and the self-quenching rate constant (Table 3). In general, the natural decay rate ( $k_0$ ) was higher in nonpolar than in polar solvents, indicating a stabilization of the lowest triplet state by the latter. The bimolecular  $k_{\text{sq}}$  was influenced more by the viscosity parameter, being higher in 3-methylpentane than in 2-propanol, as expected for an energy-transfer quenching process limited by diffusion.

#### Photophysical Parameters of the Triplet State of 1NPy.

In benzene, the value of the triplet molar absorption coefficient coincided with that reported by Sheerer and Heinglein<sup>37</sup> ( $9350 \text{ M}^{-1} \text{ cm}^{-1}$ ). Because the magnitude of the molar absorption coefficient did not change with solvent polarity, there was no change in the ordering of the triplet states. Furthermore, our results were in good agreement with the values estimated through the singlet depletion method.<sup>54</sup> Triplet yields on the order of 0.40–0.58 were determined. For these measurements, the triplet molar absorption coefficient was determined using perylene as a standard in the energy-transfer method.<sup>54</sup> The calculated values of the triplet yields were corrected for possible absorption of perylene at the wavelength of excitation of 1NPy, for the decay of the 1NPy triplet during the quenching process by perylene, and for the decay of perylene's triplet.<sup>44,54–59</sup> These values were similar to that reported by Scheerer and Henglein in benzene (0.60).<sup>37</sup> Quantum yields for triplet formation of 0.68

for 1-nitronaphthalene<sup>51,60</sup> and of 0.80 for 2-nitronaphthalene<sup>51</sup> have been reported. For 9-nitronaphthalene a triplet yield of 0.93 was estimated on the basis of a 0.07 photodestruction yield.<sup>35</sup> These values demonstrate a high intersystem crossing yield as one of the principal channels for the deactivation of the excited singlet state in nitroarenes molecules. The differences in triplet yield for the nitroarenes implied some dependence on structure or an effect of the  $\text{NO}_2$  group orientation relative to the ring system that affects the relaxation processes. Because intersystem crossing yields into the  $\pi, \pi^*$  triplet state are on the order of 0.40–0.60, and the fluorescence yields ( $10^{-4}$ ) and the internal conversion process from the singlet excited state<sup>38</sup> are insignificant pathways for the 1NPy deactivation, other deactivation channels must be considered. The postulated nitro–nitrite rearrangement from an upper ( $n, \pi^*$ ) triplet state could be a possibility. This cyclic intermediate (Scheme 1), not observed in the femtosecond transient absorption experiments,<sup>39</sup> due to its low concentration and molar absorption coefficient, could dissociate into NO (nitrogen oxide) and a pyrenoxy radical. In addition, the high energy  $n, \pi^*$  triplet state could transform into the lowest  $\pi, \pi^*$  triplet state (Table 4).

**Pyrenoxy Radical.** As stated earlier, a long-lived absorption band was seen in all solvents; although more prominently in polar solvents and at high laser energies (Figures 5 and 6). This absorption grew within the laser pulse and then slowly decayed. As previously observed for other nitroPAHs,<sup>33–36</sup> the decay of the absorption signal of the lowest triplet state was not accompanied with the simultaneous growth of the long-lived species. The signal is not seen after the depletion of the triplet state, but grows within the laser pulse. The long-lived species decayed with a half-life on the order of  $10^{-3}$  s ( $k \approx 10^3 \text{ s}^{-1}$ , assuming a first-order decay, Table 5), and its initial intensity

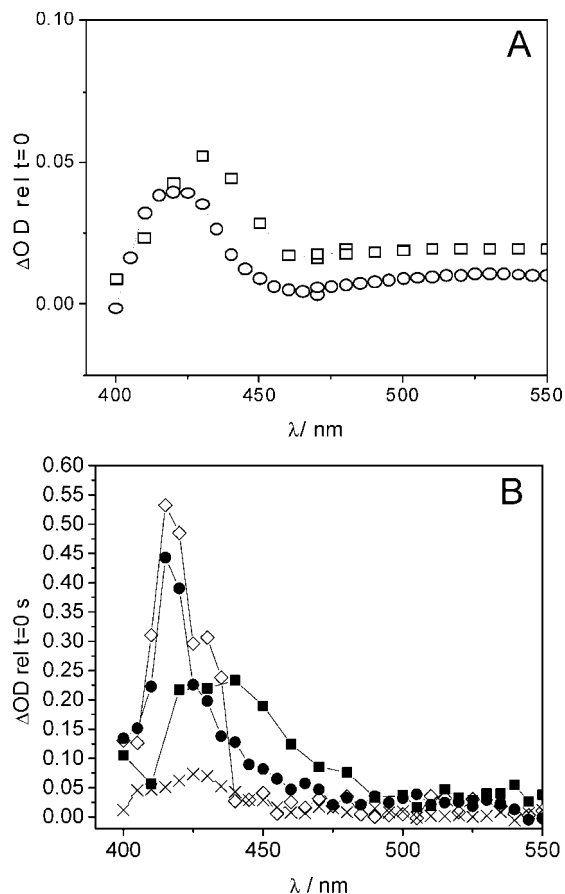


**Figure 5.** Normalized transient absorption spectra of INPy ( $6 \times 10^{-5}$  M) at long observation times ( $10^{-5}$ – $10^{-4}$  s) in nonpolar and polar solvents: (A) ( $\square$ ) cyclohexane and ( $\circ$ ) 3-methylpentane; (B) ( $\diamond$ ) acetonitrile, ( $\blacksquare$ ) methanol, ( $\bullet$ ) 2-propanol and ( $\times$ ) EPA.

was 10 times smaller than the triplet in nonpolar solvents, and one-third of the triplet in polar solvents. In both solvents, its yield showed linear dependence with the incident laser energy in the range (up to 15 mJ) where the triplet yield was also linear. Furthermore, the line passes through the origin at zero laser energy.<sup>61</sup> The wavelength of maximum absorption and the initial yield for the species both depended on solvent properties. For example, the maximum absorption wavelength was at 430 nm in cyclohexane and 440 nm in methanol. The transient spectrum observed in 2-propanol could not be completely attributed to a single long-lived transient because the maximum of the band appeared around 420 nm, and a shoulder at 440 nm suggested that an additional long-lived intermediate was generated.

To investigate the nature and possible precursors to these intermediates species, the effect of additives on their yield and decay kinetics was studied. At the highest concentration of ferrocene added ( $10^{-4}$  M), a 15–40% reduction in the yield was observed, whereas in  $O_2$ -saturated ( $10^{-3}$ – $10^{-2}$  M) solutions a greater reduction in the yield was noticed. Under  $O_2$ -saturation in solvents such as benzene, cyclohexane, 3-methylpentane,  $CCl_4$ , and acetonitrile total quenching of this species was observed, but not in  $O_2$ -saturated methanol and 2-propanol (Figure 7).

On the basis of these observations, and comparing the spectra in Figures 5 and 6 with that generated in the laser flash excitation of hydroxypyrene in methanol under  $N_2$ - and  $O_2$ -saturated conditions, and the reported spectra of the pyrenoxy ( $PyO^*$ ) radical,<sup>62,63</sup> the long-lived species is assigned to this species. Moreover, the dependence of its yield with the laser power did

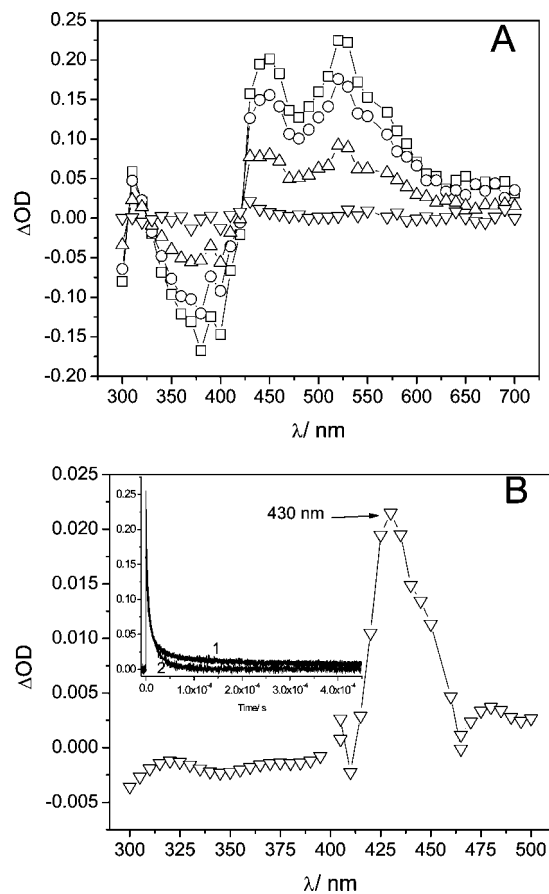


**Figure 6.** (A) Transient absorption spectra of INPy ( $6 \times 10^{-5}$  M) in cyclohexane at 0.8  $\mu$ s ( $\square$ ), 2  $\mu$ s ( $\circ$ ), 7  $\mu$ s ( $\triangle$ ), and 55  $\mu$ s ( $\nabla$ ) after the laser pulse. (B) Enlarged transient absorption spectrum at 55  $\mu$ s ( $\nabla$ ). Inset: decay kinetics at (1) 430 and (2) 550 nm. Measurements were made using high laser energies ( $\sim 50$  mJ), under  $N_2$ -saturated conditions at room temperature.

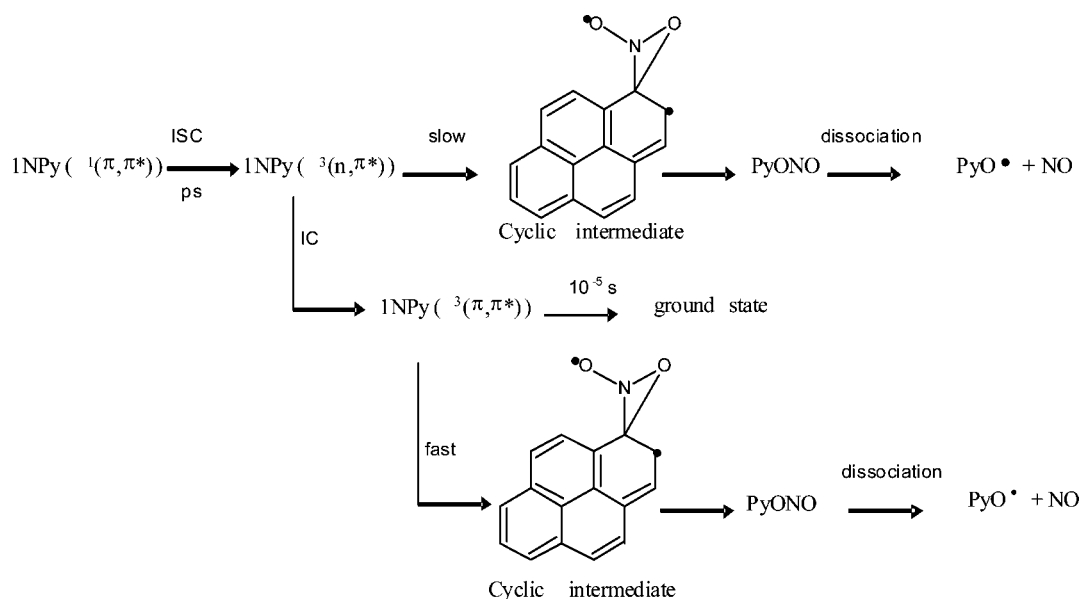
not support a multiphoton ionization process in which a INPy radical cation, an anion (formed by an electron scavenging process) or photodestruction of another intermediate could be the precursors of this species. In contrast to our results, Sheerer and Henglein<sup>37</sup> were only able to observe the long-lived intermediate in  $O_2$ -saturated solutions and no solvent effects were reported. Hamanoue et al.<sup>33</sup> previously reported that the anthryloxy radical was not produced via the lowest triplet state, because the addition of ferrocene did not affect the yield of 9-cyano-10-anthryloxy, and only slightly decreased the yield of 9-benzoyl-10-anthryloxy radicals.

Ours and others observations and interpretations in the characterization and kinetic behavior of the long-lived pyrenoxy radical deserve further attention and discussion. The participation of an aryloxy radical on the phototransformation of nitroaromatics was initially postulated in Chapman's mechanism.<sup>32</sup> It is formed from the cleavage of an aryl nitrite that results from a cyclic intermediate or transition state that participates in a nitro–nitrite rearrangement. The aryl nitrite either can thermally decompose or be photodissociated. The cyclic intermediate or the nitrite have not been detected in transient experiments most probably due to their low concentration and/or short lifetime.<sup>33–36,39,64</sup> Indeed, a photoproduct 1-hydroxypyrene resulting from a hydrogen abstraction of the pyrenoxy radical from the solvent is produced<sup>65</sup> in quantum yields on the order of  $10^{-4}$  and this yield decrease by 50% in the presence of  $O_2$ . The transient results reported herein demonstrate that the pyrenoxy radical is formed within the laser pulse simultaneously with the

**TABLE 3: Quenching, Natural Decay ( $k_o$ ) and Self Quenching ( $k_{sq}$ ) Rate Constants of Triplet State of 1NPy at Room Temperature in Solutions**

solvent	visc <sup>a</sup>	$k_q$ O <sub>2</sub> <sup>b</sup>	$k_q$ perylene <sup>b</sup>	$k_q$ <sup>c</sup>	$k_o$ <sup>c</sup>	$k_{sq}$ <sup>b</sup>
3-methylpentane	0.307	1.4 ± 0.3	18 ± 1	20 ± 1	1.0 ± 0.3	2.4 ± 0.3
cyclohexane	0.975	1.6 ± 0.1	6.4 ± 0.4	9.5 ± 0.1	1.0 ± 0.2	1.6 ± 0.2
benzene	0.649	1.6 ± 0.1	9.4 ± 0.7	10.1 ± 0.5	1.9 ± 0.3	1.9 ± 0.2
CCl <sub>4</sub>	0.969	1.3 ± 0.01		4.1 ± 0.6	0.2 ± 0.1	1.4 ± 0.1
2-propanol	2.04	1.5 ± 0.9	1.7 ± 0.2	5.2 ± 0.1	0.4 ± 0.1	1.0 ± 0.1
methanol	0.593	1.5 ± 0.2	4.4 ± 0.4	22 ± 1	0.3 ± 0.1	1.5 ± 0.1
acetonitrile	0.345	1.5 ± 0.2		16 ± 1	0.2 ± 0.1	1.4 ± 0.1

<sup>a</sup> 10<sup>-3</sup> Pa s. <sup>b</sup> 10<sup>9</sup> M<sup>-1</sup> s<sup>-1</sup>. <sup>c</sup> 10<sup>5</sup> s<sup>-1</sup>.

**SCHEME 1****TABLE 4: Triplet Molar Absorption Coefficients and Quantum Yields in Nonpolar and Polar Solvents at Room Temperature**

solvent	$\epsilon_T/10^3$ M <sup>-1</sup> cm <sup>-1</sup>	observation wavelength/nm	$\phi_{ISC}$
3-methylpentane	9.4 ± 0.8	530	0.40 ± 0.06
cyclohexane	7.8 ± 0.9	530	0.6 ± 0.1
benzene	9.2 ± 1.0	550	0.42 ± 0.06
2-propanol	9.6 ± 1.6	570	0.40 ± 0.08
methanol	6.5 ± 0.9	570	0.50 ± 0.08

**TABLE 5: Decay Rate Constant of the Long Lived Intermediate of 1NPy at Room Temperature**

solvent	observation wavelength/nm	$k_{obs}/10^4$ s <sup>-1</sup>
3-methylpentane	430	1.6 ± 0.3
cyclohexane	430	4.2 ± 0.5
benzene	430	2.2 ± 0.4
CCl <sub>4</sub>	430	0.74 ± 0.07
2-propanol	430	0.68 ± 0.04
methanol	430	0.28 ± 0.07
acetonitrile	430	0.65 ± 0.05

$\pi,\pi^*$  triplet state. Its yield decreased significantly in the presence of triplet quenchers (O<sub>2</sub>, ferrocene), although its lifetime was not affected. These intriguing results could be implying a triplet precursor to this species. In Chapman's mechanism the triplet-state precursor was postulated to be a  $n,\pi^*$  triplet state. This state then relaxes by two competing channels, one leading to the lowest  $\pi,\pi^*$  triplet state, and the other to the cyclic intermediate. The only way that a triplet quencher could induce a decrease in the yield of the cyclic intermediate would be if

the rate constant for the rearrangement of the  $n,\pi^*$  triplet state is small enough for the quenchers to deactivate this state by a diffusion controlled process. Still another possibility, suggested by Zewail et al.<sup>64</sup> in the case of nitrobenzene, is that the  $\pi,\pi^*$  triplet state is the precursor, and that this state could also deactivate through two parallel channels, one a very fast rearrangement leading to the pyrenoxy radical, and a second one relaxing to the ground state. In this case, the triplet quenchers could deactivate the long-lived  $\pi,\pi^*$  triplet state and the observed results could be rationalized (Scheme 1).

**Quenching of the  $\pi,\pi^*$  Triplet State of 1NPy by Phenols.**

To test the hypothesis that the hydrogen abstraction reaction by the 1NPy triplet state is one of the major decay processes in the photochemistry of nitroarenes in the organic phase of the atmospheric aerosols, 1NPy was excited in the presence of phenolic compounds (ArOH) acting as hydrogen donors in cyclohexane, acetonitrile, and 2-propanol. Hydroxy-PAHs present in diesel exhaust<sup>23-25</sup> or formed in the atmosphere were chosen for this purpose. Also, used as hydrogen donors were *o*-methoxyphenols as important constituents of wood smoke aerosols.<sup>23-25</sup> The solvents used were selected as an attempt to mimic polar protic and aprotic and nonpolar compounds in aerosols. In the concentration range used for the ArOH derivatives these did not show a significant absorption at the excitation wavelength of 355 nm. Furthermore, the ground-state absorption spectra did not demonstrate the appearance of isosbestic points or new bands, indicating that the ground state of 1NPy did not form a ground-state complex with the ArOH. However, the 1NPy triplet state lifetime decreased with increasing ArOH concentration. The triplet decay fitted to a monoex-

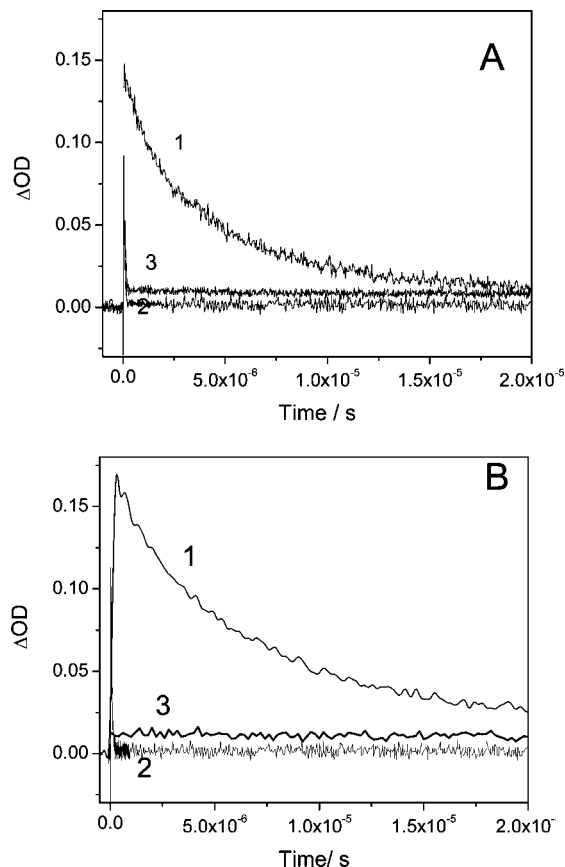


**Figure 7.** Decay kinetics of intermediates of INPy in (A) methanol and (B) 2-propanol. Typical triplet decay at 550 nm in the (1) absence and (2) the presence of oxygen. (3) Long-lived species decay monitored at 430 nm under  $O_2$ -saturated conditions.

**TABLE 6: Quenching Rate Constants of the  $\pi,\pi^*$  Triplet State of INPy by ArOH**

phenolic compound	$k_q^{ArOH}/10^9 \text{ M}^{-1} \text{ s}^{-1}$		$E_{ox}^{ENH}/V$
	cyclohexane	acetonitrile	
phenol	$0.13 \pm 0.03$	$0.05 \pm 0.01$	$0.898^a$
1,2-dihydroxybenzene		$0.20 \pm 0.01$	$0.502^b$
1,4-dihydroxybenzene		$0.24 \pm 0.01$	$0.421^b$
1,2,4-trihydroxybenzene		$2.2 \pm 0.1$	
1-hydroxynaphthalene	$6.1 \pm 0.2$	$0.32 \pm 0.02$	$0.590^c$
2-hydroxynaphthalene	$1.0 \pm 0.1$		
4-hydroxy-3-methoxybenzoic acid		$0.016 \pm 0.009$	$0.998^d$
2,6-dimethoxyphenol	$0.25 \pm 0.02$	$0.20 \pm 0.01$	$0.693^a$
4-hydroxy-3-methoxybenzaldehyde		$0.046 \pm 0.005$	$0.888^a$
3-methoxy-4-hydroxyphenyl acetic acid	$0.18 \pm 0.05$	$0.32 \pm 0.04$	

<sup>a</sup> Data from ref 66. <sup>b</sup> Reference 67. <sup>c</sup> Reference 68. <sup>d</sup> Reference 69. The reduction potential of INPy ( $-0.485 \text{ V}$ ) was obtained from ref 70.

ponential decay in the presence of the phenolic compounds. The quenching rate constants were calculated from Stern–Volmer plots (Table 6). All values were under the diffusion limit.

Hydrogen abstraction reactions by  $n,\pi^*$  and  $\pi,\pi^*$  carbonyl triplets occur by different mechanisms depending on the properties of the hydrogen donor and the triplet state.<sup>71–74</sup> These mechanisms go from pure alkoxy radical like abstractions to the other extreme of one initiated by full electron transfer to the excited carbonyl triplet from the hydrogen donor. The latter case has been observed for nitroaryl triplet in the presence of amines.<sup>37,75</sup> Our laser flash results did not provide evidence for

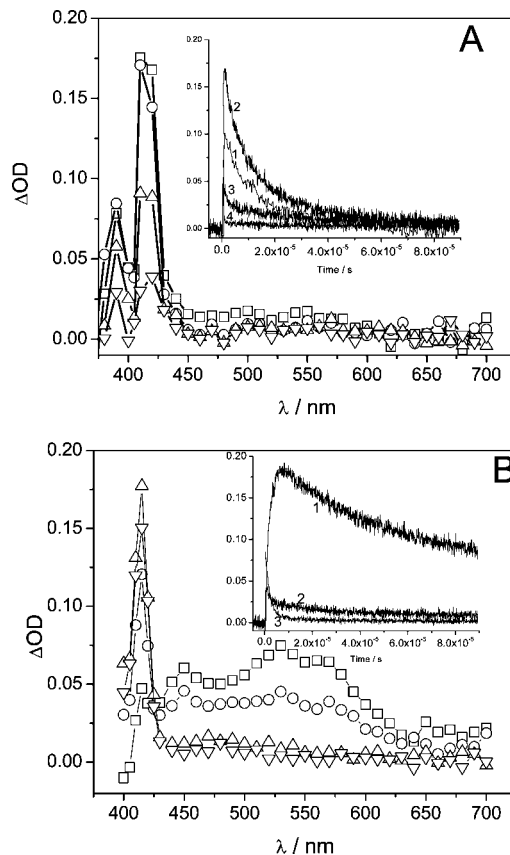


**Figure 8.** Transient absorption spectra of INPy solutions ( $6 \times 10^{-5} \text{ M}$ ) containing 1-hydroxynaphthalene ( $7.5 \times 10^{-4} \text{ M}$ ). In (A) cyclohexane. Inset: decay kinetics at (1) 390, (2) 420, (3) 430, and (4) 530 nm. (B) In acetonitrile. Inset: decay kinetics at (1) 420, (2) 430, and (3) 550 nm. Under  $N_2$ -saturated conditions at  $0.8 \mu\text{s}$  ( $\square$ ),  $2 \mu\text{s}$  ( $\circ$ ),  $7 \mu\text{s}$  ( $\Delta$ ), and  $20 \mu\text{s}$  ( $\nabla$ ) after the laser pulse.

a complete electron transfer because we did not observe a transient signal corresponding to the nitropyrene radical anion. However, the large magnitude ( $10^7$ – $10^9 \text{ M}^{-1} \text{ s}^{-1}$ ) for the rate constants obtained for the quenching of the lowest triplet state of INPy by hydrogen donors could be explained if the hydrogen abstraction reaction goes through an electron transfer within a hydrogen-bonded triplet exciplex followed by a proton-transfer mechanism.<sup>71–74</sup> A plot of  $\log k_q^{ArOH}$  versus the oxidation potential of the ArOH ( $E_{ox}^{ArOH}$ ) showed a Rehm–Weller behavior in acetonitrile (data not shown). This result supports an electron-transfer process in the quenching of the lowest triplet state of INPy by aromatic hydrogen donors. Furthermore, the differences in rate constants observed in the different solvents could be explained by the importance of the formation of strong hydrogen bonds in the reactive site.<sup>71</sup>

In the wavelength region below 430 nm, an increase in the initial absorbance with increasing ArOH concentration was observed as the triplet initial concentration decreased. The presence of ArOH had no noticeable effect on the rate of decay of the long-lived absorption.

Transient absorption spectra were obtained for laser-irradiated solutions of INPy in cyclohexane and acetonitrile containing 1-hydroxynaphthalene at a concentration of  $7.5 \times 10^{-4} \text{ M}$  under He-saturated conditions (Figure 8). These present an initial spectrum that resembles the one observed for INPy in the pure solvents. Nonetheless, at longer observation times, when no triplet absorption was noticeable, the spectrum in cyclohexane showed two strong-sharp bands with maxima at 390 and 425 nm, respectively, which grew as a function of observation time.



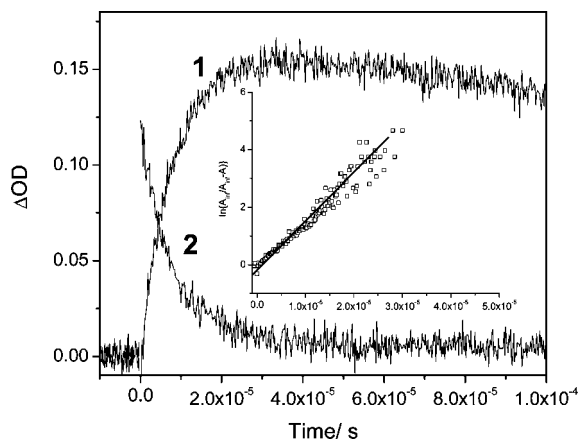


**Figure 9.** Kinetic decay under  $N_2$ -saturated conditions of a 1NPy ( $6 \times 10^{-5}$  M) solution with 1-hydroxynaphthalene ( $3.25 \times 10^{-5}$  M) in 2-propanol monitored at (1) 425 and (2) 550 nm. The inset shows the fit of 425 nm absorption data to  $\ln[A_0/A_\infty - A_0]$  vs time.

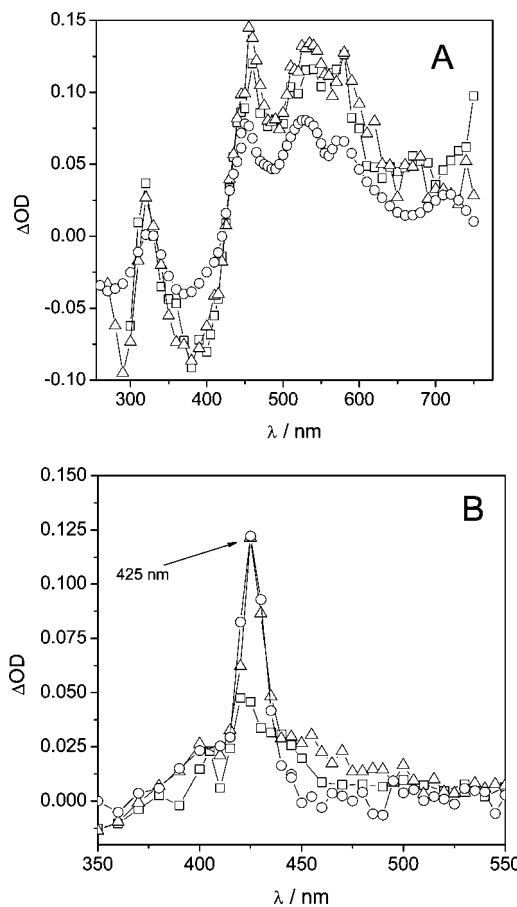
The spectrum was different from that observed for the pyrenoxy radical in this solvent ( $\lambda_{\max}$ , 420 nm; bandwidth, 50 nm). The band with maxima at 390 nm was characteristic of the 1-naphthalenoxy radical<sup>76</sup> which has a molar absorption coefficient of  $4830 \text{ M}^{-1}\text{cm}^{-1}$ . Thus, the second band at 425 nm ( $\epsilon = 1.03 \times 10^4 \text{ M}^{-1}\text{cm}^{-1}$ ) was assigned to the radical formed from the reaction of the 1NPy triplet state with the hydrogen donor (process 2.15 in Scheme 2). In support of this assignment, the decay rate constant of this long-lived species was around 2 times higher than for the pyrenoxy radical, and the rate constant for the growth of the 425 nm absorption (Figure 9) was similar to that calculated for 1NPy triplet decay ( $10^6 \text{ s}^{-1}$ ).

Figure 10 shows transient spectra obtained in neat 2-propanol and in the presence of 1-hydroxynaphthalene and 2,6-dimethoxyphenol at short and long observation times. In both cases, the spectrum observed at long observation times showed an increase in the absorption at 425 nm while the triplet state was decaying. This could be attributed to the presence of  $(\text{PyNO}_2\text{H})^\bullet$  in solvents with the ability to donate hydrogen. It was also in agreement with previous reports on C–H hydrogen abstraction in this solvent by 2-nitronaphthalene.<sup>77</sup>

Feilberg and Nielsen<sup>25</sup> observed acceleration in the photodegradation of 1NPy in the presence of phenolic aerosol constituents, especially for 1- and 2-hydroxynaphthalenes. Minor or no effects were observed in the presence of phenol or methoxyphenols. Our transient results indicated that phenol and methoxyphenols quench the 1NPy triplet state with a rate constant an order of magnitude lower than the hydroxynaphthalenes agreeing with their results. They proposed<sup>25</sup> that the increase in the photodegradation of 1NPy in the presence of phenolic compound could be due to a hydrogen abstraction of the phenolic hydrogen by  $^3\text{1NPy}$  or to the photodissociation of the phenolic O–H bond. Because the tested phenols do not absorb at the wavelength of laser excitation (355 nm), our results clearly indicated that the increase in the photodegradation rate was due to hydrogen abstraction reaction via coupled electron–proton transfer, which can initiate radical reactions.<sup>25</sup>

## Conclusions

The photophysical and photochemical properties of 1-nitropyrene, the most abundant nitro-PAH in diesel exhaust, depend largely on solvent properties such as polarity, viscosity, and hydrogen donor abilities. Strong solvent interactions were reflected by changes in the bandwidth, the relative intensities



**Figure 10.** Transient absorption spectra under  $N_2$ -saturated conditions of (A) ( $\square$ ) 1NPy solutions ( $6 \times 10^{-5}$  M) in 2-propanol, with ( $\circ$ ) 2,6-dimethoxyphenol ( $1 \times 10^{-4}$  M), and ( $\triangle$ ) 1-hydroxynaphthalene ( $3.25 \times 10^{-5}$  M) at  $0.8 \mu\text{s}$ , and (B) spectra  $1.79 \times 10^{-4}$  s after the laser pulse.

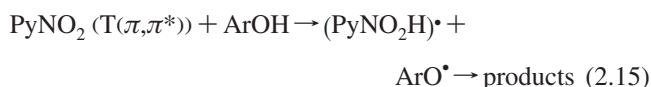
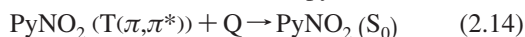
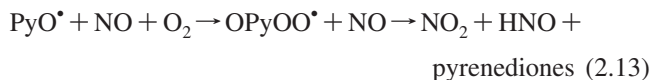
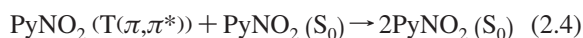
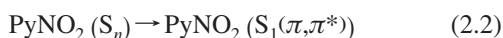
of the vibronic bands, oscillator strengths, and absorption maxima of the ground-state absorption band associated with the  $\text{NO}_2$  group chromophore. Our, low fluorescence yields ( $10^{-4}$ ), reduced internal conversion yield from the excited singlet,<sup>48</sup> and calculations<sup>39</sup> suggested a strong spin–orbit coupling and higher intersystem crossing yields into an upper  $^3(n,\pi^*)$ . This state rapidly relaxes into a low energy  $^3(\pi,\pi^*)$  state with yields of 0.40–0.60, suggesting other singlet or higher triplet state deactivation routes. Low temperature phosphorescence, and transient spectra resulting from the 266 or 355 nm nanosecond laser excitation, indicated the presence of a low lying  $^3(\pi,\pi^*)$  that decayed with lifetimes of  $10^{-5}$ – $10^{-4}$  s at room temperature. The attribution to the pyrenoxy radical to a long-lived species that grows within the laser pulse, was corroborated by a comparison of its narrow band spectrum with maximum at 420–430 nm with published spectra for this radical. This intermediate has been postulated to arise from a nitro–nitrite rearrangement with subsequent dissociation into the pyrenoxy radical and  $\text{NO}$ .<sup>32</sup> The effect of triplet quenchers on the absorption of the long-lived species suggested that it could also be formed from the  $^3(\pi,\pi^*)$  state,<sup>64</sup> in addition to the postulated  $^3(n,\pi^*)$  precursor. The lowest energy triplet state reacts readily with hydrogen donors to form the  $\text{PyNO}_2\text{H}$  radical. This long-lived transient was clearly detected in 2-propanol, where a hydrogen abstraction reaction is also possible.

Photodestruction yields of 1NPy in these solvents<sup>65</sup> range from  $1.4 \times 10^{-3}$  in polar protic (methanol, 2-propanol, EPA) to  $(1.7 \text{ to } 3.9) \times 10^{-4}$  in nonpolar hexane and 3-methylpentane.

Hydroxypyrene, one of the principal products, made up approximately 50% of the photodestruction yields. This product was formed from reactions of the pyrenoxy radical with the solvent, and as expected was not observed in CCl<sub>4</sub>, toluene, or benzene. The small magnitude of the photoreaction yields (10<sup>-3</sup>–10<sup>-4</sup>) compared to the intersystem crossing yield into the <sup>3</sup>(π,π\*) state and the small effect of O<sub>2</sub> on the photodestruction yield suggest that this state contributes very little to the photoreaction. The larger yield of photodestruction in polar protic solvents implied a greater contribution from a <sup>3</sup>(π,π\*) hydrogen atom abstraction reaction.

The small yield of photoreduction also suggested that the pyrenoxy radical had little reactivity, possibly due to its possible recombination with NO in the solvent cage to regenerate the parent compound. Our results as well as from others are summarized in Scheme 2.1:

### Scheme 2



Q = O<sub>2</sub>, ferrocene, perylene; RH = ArOH or 2-propanol; and radical-radical termination reactions are not included in this scheme.

In terms of the environmental photochemical implications of these results, although the principal degradation pathways of nitroPAHs found in the atmospheric particulate matter appear to be photodegradation, the low reactivity of the photochemical intermediates could explain their persistence in the environment. Our results suggest that the reactivity of INPy and its intermediates depends on the microenvironment in the aerosol and that the major photochemical reactions of this pollutant will be with other major organic constituents in the aerosol. The major product, hydroxypyrene, although formed in low yields, has demonstrated adverse health effects in humans.

**Acknowledgment.** We acknowledge the financial support from NIH SCoRE (5S06GM08102). We thank Dr. C. Crespo of Case Western University for his helpful comments.

### References and Notes

- (1) Tong, H. Y.; Karasek, F. W. *Anal. Chem.* **1984**, *56*, 2129.
- (2) Finlayson-Pitts, B. J.; Pitts, J. N., Jr. *Science* **1997**, *276*, 1045.
- (3) Yang, H. H.; Lai, S. O.; Hsieh, L. T.; Hsueh, H. J.; Chi, T. W. *Chemosphere* **2002**, *48*, 1061.
- (4) Hayakawa, K.; Murahashi, T.; Butoh, M.; Miyazaki, M. *Environ. Sci. Technol.* **1995**, *29*, 928.
- (5) Tang, N.; Hattori, T.; Taga, R.; Igarashi, K.; Yang, X.; Tamura, K.; Kakimoto, H.; Mishukov, V. F.; Toriba, A.; Kizu, R.; Hayakawa, K. *Atmos. Environ.* **2005**, *39*, 5817.
- (6) Arey, J.; Zielinska, B.; Atkinson, R.; Winer, A. M.; Ramdahl, T.; Pitts, J. N. *Atmos. Environ.* **1986**, *20*, 2339.
- (7) Ciccioli, P.; Cecinato, A.; Brancaleoni, E.; Frattoni, M.; Zacchei, P.; Miguel, A. H.; Vasconcelos, P. de C. *J. Geophys. Res.* **1996**, *101*, 19567.
- (8) Chan, P. C. *NTP technical report, National Toxicology Program, U.S. Department of Health and Human Services, NIH publication 1996*, *96*, 3383.
- (9) Ardent Pope, C., III; Burnett, R. T., III; Thun, M. J.; Calle, E. E.; Krewski, D.; Ito, K.; Thurston, G. D. *J. Am. Med. Assoc.* **2002**, *287*, 1132.
- (10) Bamford, H. A.; Bezabeh, D. Z.; Shantz, M. M.; Wise, S. A.; Baker, J. E. *Chemosphere* **2003**, *50*, 575.
- (11) Hayakawa, K.; Tang, N.; Akutsu, K.; Murahashi, T.; Kakimoto, H.; Kizu, R.; Toriba, A. *Atmos. Environ.* **2002**, *36*, 5535.
- (12) Rosenkranz, H. S.; Mermelstein, R. *Mutat. Res.-Genet. Tox.* **1983**, *114*, 217.
- (13) Chae, Y. -H.; Upadhyaya, P.; Ji, B. -Y.; Fu, P. P.; El-Bayoumy, K. *Mutat. Res.-Fundam. Mol. Mechanisms Mutagenesis* **1997**, *376*, 21.
- (14) Topinka, J.; Schwarz, L. R.; Kiefer, F.; Wiebel, F. J.; Gajdoš, O.; Vidová, P.; Dobiáš, L.; Fried, M.; Šrám, R. J.; Wolff, T. *Mutat. Res.-Genet. Tox.* **1998**, *419*, 91.
- (15) Taga, R.; Tang, N.; Hattori, T.; Tamura, K.; Sakai, S.; Toriba, A.; Kizu, R.; Hayakawa, K. *Mutat. Res.-Genet. Tox. Environ.* **2005**, *581*, 91.
- (16) Enya, T.; Susuki, H.; Watanabe, T.; Hirayama, T.; Hisamatsu, Y. *Environ. Sci. Technol.* **1997**, *31*, 2772.
- (17) Kamens, R. M.; Zhi-Hua, F.; Yao, Y.; Chen, D.; Chen, S.; Vartiainen, M. *Chemosphere* **1994**, *28*, 1623.
- (18) Fan, Z.; Chen, D.; Birla, P.; Kamens, R. M. *Atmos. Environ.* **1995**, *29*, 1171.
- (19) Fan, Z.; Kamens, R. M.; Hu, J.; Zhang, J.; McDow, R. S. *Environ. Sci. Technol.* **1996**, *30*, 1358.
- (20) McDow, S. R.; Sun, Q.; Vartiainen, M.; Hong, Y.; Yao, Y.; Fister, T.; Yao, R.; Kamens, R. M. *Environ. Sci. Technol.* **1994**, *28*, 2147.
- (21) McDow, R. S.; Vartiainen, M.; Sun, Q.; Hong, Y.; Yao, Y.; Kamens, R. M. *Atmos. Environ.* **1995**, *29*, 791.
- (22) McDow, S. R.; Jang, M.; Hong, Y.; Kamens, R. M. *J. Geophys. Res.* **1996**, *101*, 19593.
- (23) Jang, M.; McDow, S. R. *Environ. Sci. Technol.* **1995**, *29*, 2654.
- (24) Feilberg, A.; Nielsen, T. *Environ. Sci. Technol.* **2000**, *34*, 789.
- (25) Feilberg, A.; Nielsen, T. *Environ. Sci. Technol.* **2001**, *35*, 108.
- (26) Van den Braken-van Leersum, A. M.; Tintel, C.; van't Zelfde, M.; Cornelisse, J.; Lugtenburg, J. *Recl. Trav. Chim. Pays-Bas* **1987**, *106*, 120.
- (27) Stärk, G.; Stauff, J.; Miltenburger, H. G.; Stumm-Fisher, I. *Mutat. Res.-Genet. Tox.* **1985**, *155*, 27.
- (28) Holloway, M. P.; Biaglow, M. C.; McCoy, E. C.; Anders, M.; Rosenkranz, H. S.; Howard, P. C. *Mutat. Res.-Genet. Tox.* **1987**, *187*, 199.
- (29) Koizumi, A.; Saitoh, N.; Susuki, T.; Kamiyama, S. *Arch. Environ. Health* **1994**, *49*, 87.
- (30) Muck, A.; Kubát, P.; Oliviera, A.; Ferreira, L. F. V.; Cvacka, J.; Civi, S.; Zelinger, Z.; Barek, J.; Zima, J. *J. Hazard. Mater.* **2002**, *95*, 175.
- (31) Warner, S. D.; Farant, J. P.; Butler, I. S. *Chemosphere* **2004**, *54*, 1207.
- (32) Chapman, O. L.; Heckert, D. C.; Reasoner, J. W.; Thackaberry, S. P. *J. Am. Chem. Soc.* **1966**, *88*, 5550.
- (33) Hamanoue, K.; Amano, M.; Kimoto, M.; Kajiwara, Y.; Nakayama, T.; Teranishi, H. *J. Am. Chem. Soc.* **1984**, *106*, 5993.
- (34) Hamanoue, K.; Nakayama, T.; Ushida, K.; Kajimara, K.; Yamanaka, S. *J. Chem. Soc., Faraday Trans.* **1991**, *87*, 3365.
- (35) Hamanoue, K.; Nakayama, T.; Kajiwara, K.; Yamanaka, S.; Ushida, K. *J. Chem. Soc., Faraday Trans.* **1992**, *88*, 3145.
- (36) Hamanoue, K.; Nakayama, T.; Amijima, Y.; Ibuki, K. *Chem. Phys. Lett.* **1997**, *267*, 165.
- (37) Scheerer, R.; Henglein, A. *Ber. Bunsen-Ges. Phys. Chem.* **1977**, *81*, 1234.
- (38) Morales-Cueto, R.; Esquivelzeta-Rabell, M.; Saucedo-Zugazagoitia, J.; Peón, J. *J. Phys. Chem. A* **2007**, *111*, 552.
- (39) Crespo-Hernández, C.; Burdzinski, G.; Arce, R. *J. Phys. Chem. A* **2008**, *112*, 6313.
- (40) Güsten, H.; Heinrich, G. *J. Photochem.* **1982**, *18*, 9.
- (41) Fiorelli, S.; Arce, R. *J. Phys. Chem. A* **2003**, *107*, 5968.
- (42) Arce, R.; García, C.; Oyola, R.; Piñero, L.; Nieves, I.; Cruz, N. *J. Photochem. Photobiol. A Chem.* **2003**, *154*, 245.
- (43) Bensasson, R.; Land, E. *J. Trans. Faraday Soc.* **1971**, *67*, 1904.
- (44) Cosa, G.; Scaiano, J. C. *Photochem. Photobiol.* **2004**, *80*, 159.
- (45) Klessinger, M.; Michl, J. *Excited states and photochemistry of organic molecules*; VCH Publishers, Inc.: Berlin, 1995; Vol. 2, p 134.

- (46) Wolfbeis, O. S.; Posch, W.; Gübitz, G.; Tritthart, P. *Anal. Chem. Acta* **1983**, *147*, 405.
- (47) Gilbert, A.; Baggot, J. *Essentials of molecular photochemistry*; Blackwell Scientific Publications: Oxford, U.K., and Boston, 1991; Vol. 3, p 85.
- (48) Guilbault, G. *Practical fluorescence*; Marcel Dekker, Inc.: New York, 1990; p 97.
- (49) Hirayama, S.; Kajiwara, Y.; Nakayama, T.; Hammoue, K.; Teranishi, H. *J. Phys. Chem.* **1985**, *89*, 1945.
- (50) Mikula, J. J.; Anderson, R. W.; Harris, L. E. *Adv. Mol. Relaxation Process* **1973**, *5*, 193.
- (51) Rusakowicz, B.; Testa, A. C. *Spectrochim. Acta A: Mol. Spectrosc.* **1971**, *27*, 787.
- (52) Herkstroeter, W. G. *J. Am. Chem. Soc.* **1975**, *97*, 4161.
- (53) Murov, S. L.; Carmichael, I.; Hug, G. L. *Handbook of Photochemistry*; Marcel Dekker, Inc.: New York, 1993; Vol. 107, p 109.
- (54) Bonneau, R.; Carmichael, I.; Hug, G. L. *Pure Appl. Chem.* **1991**, *63*, 289.
- (55) Amouyal, E.; Bensasson, R. *Photochem. Photobiol.* **1974**, *20*, 415.
- (56) Amand, B.; Bensasson, R. *Chem. Phys. Lett.* **1975**, *34*, 44.
- (57) Bensasson, R.; Goldschmidt, C. R.; Land, E. J.; Truscott, T. G. *Photochem. Photobiol.* **1977**, *28*, 277.
- (58) Carmichael, I.; Hug, G. L. *J. Phys. Chem. Ref. Data* **1986**, *15* (1), 1–250.
- (59) Bensasson, R.; Land, E. J.; Truscott, T. G. *Excited states and free radicals in biology and medicine: contributions from flash photolysis and pulse radiolysis*; Oxford University Press: New York, 1993; Chapter 5, p 77.
- (60) Hurley, R.; Testa, A. C. *J. Am. Chem. Soc.* **1968**, *90*, 1949.
- (61) Lachish, U.; Shafferman, A.; Stein, G. *J. Chem. Phys.* **1976**, *64*, 4205.
- (62) Milosavljevic, B. H.; Thomas, J. K. *Photochem. Photobiol. Sci.* **2002**, *1*, 100.
- (63) Mori, Y.; Shinoda, H.; Nakano, T.; Takasu, R.; Kitagawa, T. *J. Photochem. Photobiol. A: Chem.* **2006**, *182*, 168.
- (64) He, Y.; Gahlamann, A.; Feenstra, J. S.; Park, S. T.; Zewail, A. H. *Chem. Asian J.* **2006**, *1*, 56.
- (65) García, Z.; Arce, R. Unpublished results.
- (66) Bortolomeazzi, R.; Sebastianutto, N.; Toniolo, R.; Pizzariello, A. *Food Chem.* **2007**, *100*, 1481.
- (67) Simiã, A.; Manojloviã, D.; Cægan, D.; Todoroviã, M. *Molecules* **2007**, *72*, 2327.
- (68) Born, M.; Carrupt, P.-A.; Zini, R.; Brée, F.; Tillement, J.-P.; Hostettmann, K.; Testa, B. *Helv. Chim. Acta* **1996**, *79*, 1147.
- (69) Das, N. T.; Neta, P. A. *J. Phys. Chem. A* **1998**, *102*, 7081.
- (70) Lopes, W. A.; Pereira, P. A. de P.; Viertler, H.; de Andrade, J. B. *J. Braz. Chem. Soc.* **2005**, *16*, 1099.
- (71) Das, P. K.; Encinas, M. V.; Scaiano, J. C. *J. Am. Chem. Soc.* **1981**, *103*, 4154.
- (72) Leigh, W. J.; Lathioor, E. C.; Pierre, M. J. *St. J. Am. Chem. Soc.* **1996**, *118*, 12339.
- (73) Yoshihara, T.; Yamaji, M.; Itoh, T.; Shikuza, H.; Shimokage, T.; Tero-Kubota, S. *Phys. Chem. Chem. Phys.* **2000**, *2*, 993.
- (74) Yamaji, M.; Itoh, T.; Tobita, S. *Photochem. Photobiol. Sci.* **2002**, *1*, 869.
- (75) Görner, H. *J. Phys. Chem. A* **2002**, *106*, 5989.
- (76) Das, P. K.; Encinas, M. V.; Steenken, S.; Scaiano, J. C. *J. Am. Chem. Soc.* **1981**, *103*, 4162.
- (77) Obi, K.; Bottenheim, J. W.; Tanaka, I. *Bull. Chem. Soc. Jpn.* **1973**, *46*, 1060.

JP803051X